

CARBON DIOXIDE CAPTURE WITH POTASSIUM CARBONATE FOR NAVAL APPLICATIONS

M. Balsamo, A. Erto, A. Lancia and F. Di Natale

Dipartimento di Ingegneria Chimica, dei Materiali e della Produzione Industriale, Università di Napoli "Federico II", P.le Tecchio 80, 80125 Napoli, Italia, marco.balsamo@unina.it

ABSTRACT

In this paper, we report preliminary results on the removal of CO₂ from a model engine exhaust of marine diesel by means of K₂CO₃. The current experimental campaign belongs to a wider research framework aimed at the use of alkali-based carbonates for ship on-board Carbon Capture and Storage systems. This represents a valid solution for carbon dioxide capture to circumvent the common drawbacks associated with amine-based absorbents.

Continuous adsorption tests have been carried with a commercial potassium carbonate sorbent in a fixed bed column by treating a 5/5/90% by vol. CO₂/water vapour/N₂ mixture at 60, 75, 90 and 105°C. Outcomes highlighted that a greater CO₂ capture efficiency can be obtained at 60°C due to the exothermic nature of the process, while for temperatures greater than 90°C the carbonation degree is strongly reduced. Moreover, the evaluation of the average capture efficiency suggests that a capture step up to 300 s allows a better exploitation of the sorbent capture ability due to a significant slow-down of the carbonation rate observed for longer time.

Regeneration studies conducted at 120, 150, 200°C, after sorbent saturation at 60°C, allowed identifying the more suitable thermal conditions for CO₂ recovery. At 150°C, CO₂ can be recovered at higher concentration than the CO₂-polluted stream with a relatively fast kinetics and simultaneously ensuring a minimal reduction of the sorbent capture ability (18%) after five adsorption-desorption cycles. On the other hand, desorption temperatures greater than 200°C strongly compromise the sorbent regenerability due to a significant loss of its total porosity and surface area.

Keywords: Carbon capture and storage, Solid-gas reaction study, Sorbent regeneration.

1. INTRODUCTION

Carbon dioxide emissions are recognized among the major climate forcing agent. This is not due to its absolute intrinsic radiative index, but rather to the extension of its worldwide emissions.

Following the Kyoto and the Copenhagen protocols, many national governments, among which those of the European Union, agreed with a reduction of the carbon dioxide emissions. In its White Book on Transport (2011), the European Union indicated for maritime shipping the target of 40% low-carbon fuels by 2050 (Waterborne, 2011 and 2012). The emissions of CO₂ are strictly correlated with the efficiency of the energy production system. Therefore, more efficient systems mean less CO₂ emission.

In order to improve ship efficiency and, consequently, to reduce CO₂ emissions, the International Maritime Organization (IMO) introduced different measures, among which the Energy Efficient Design Index, EEDI, (International Maritime Organization, 2009 and 2014). The approach lying behind the EEDI is to establish a roadmap toward a progressive reduction of ship emissions and energy consumption compared to 2008, taken as reference. A time route for the EEDI energy reduction percentages was established for each class of ships, starting from the new units built from 01.01.2013 and organized in three time-steps: 0-10% for ships built within 01.01.2013 and 31.12.2019; 10-20% from 01.01.2020 to 31.12.2024 and 20-30% after 01.01.2025.

The EEDI is calculated according to a specific algorithm (International Maritime Organization, 2009 and 2014) that considers six main components:

- Ship design architecture

- Main propulsion system
- Auxiliary energy systems
- Alternative propulsion system and energy recovery units
- Fuel type
- Routing and optimal operational procedures (SEEMP)

Among them, the fuel type contribution is meant as a measure of the C/H ratio, which correlates fuel consumption to CO₂ emissions.

Ship design architecture, design of auxiliary systems, alternative propulsion systems and routing and optimal operations can reduce energy consumption and, in parallel CO₂ emissions. Among them, only slow steaming and weather routing can achieve an increase in energy efficiency up to 30-40%, while ship design modifications may achieve reductions up to 15% especially for new vessels. A summary of different strategies to improve ship emissions is reported in Table 1 which was adapted from the review of Di Natale and Carotenuto (2015).

Exhaust gas cleaning units may provide appreciable removal of CO₂, but several hindrances limit the direct extension of land-based processes to marine applications. For example, the wide experience in absorption processes, based on monoethanol- or diethanol-ammines (MEA and DEA), although conceptually applicable on-board ships, has several problems that limits its full scale application.

The applicability of Carbon Capture and Storage (CCS) system was demonstrated by DNV and PSE in 2012 (DNV-GL, 2013) using scrubbers with MEA solutions. However, the energy requirement for solvent regeneration is about 60% of the total energy consumption.

Moreover, the high costs related to the temperature required to desorb the CO₂ form the liquid, to the degradation of the amines, and to the liquid pumping, and the toxicity of process by-products, are some of the most relevant problems.

Table 1: Summary of processes for energy recovery and CO₂ reductions onboard ships.

Strategy	Potential CO₂ reduction
ENERGY EFFICIENT OPERATIONS	
Slow steaming	15-40
Weather routing	20-30
Advanced routing	2-4
Optimal cargo handling	1-5
Optimal berthing, mooring and anchoring	1-2
SHIP DESIGN	
Ship's architecture	
Ballast water and trimming optimization	1-5
Plant design	1-4
Propeller design optimization	
- Propeller upgrade (nozzle and tip winglets)	0.5-3%
- Propeller boss cap with fins	1-3%
- Complete propeller-rudder replacement	2-6%
Weight reduction	<5%
Air lubrication	
- Tanker/bulker	10-15%
- Container	5-9%
- Fishing boats	1-4%
Aerodynamics	3-4%
Hull coating	0.5-9%
Hull cleaning	1-10%
Power train optimization	<2%
Optimal hull design	5-20%
Advanced autopilot	0.5-3%
Auxiliaries	

Pumps and fan velocity control	<1%
Machinery monitoring	0.5-1%
Alternative propulsion system and energy recovery units	
Hybrid battery and diesel–electric main propulsion system	<30%
Waste heat recovery	5-15%
Waste heat recovery with organic ranking cycle	6-9%
High efficient lightning	<1%
Solar energy	2-10%
Wind assistance (sails/kites)	2-32%
Wind assistance (Flettner rotors)	3.5-12.5%
ENGINE MODIFICATIONS	
Slow steaming with engine de-rating	1-4
Main engine retrofit - tuning	0.1-0.8%
Improved gear system	8-15%

In this scenario, our research group is developing a new process for CO₂ capture by means of environmentally friendly carbonate-based sorbents able to effectively reduce CO₂ emissions by conversion into bicarbonates at low temperatures (60-100°C) and high humidity environments. These conditions are typical of the gas flowing out the conventional scrubbers used for SO₂ reduction. Besides, the process target, based on preliminary calculations is trying to operate the system with almost half the energy required for MEA scrubbing. After the treatment, the sorbent can be regenerated to recover CO₂ as an almost pure gas to be stored as a liquid in cryogenic tank. The CCS concept include liquefaction of CO₂ at 6.5 bar and -52°C for disposal at docks. In a carbon trading market, with an average price of \$20 per ton of CO₂, this disposal can represent an additional valuable income. Assuming a target removal efficiency of 30%, the amount of liquid CO₂ to be stored is 0.3 T/MWh

In this study we are reporting preliminary results to assess the conversion rate of potassium carbonate and to provide indications on the recovery rate and desorption efficiency of the CO₂.

2. MATERIALS AND METHODS

2.1 K₂CO₃ SORBENT

The porous material selected for CO₂ adsorption tests is a commercially available potassium carbonate (supplied by Carlo Erba Reagents). The raw K₂CO₃ was mechanically sieved in the range 300-630 μm so to obtain sorbent particles ensuring low pressure drops ($\approx 10^{-3}$ bar) across the fixed bed reactor. The sorbent porosimetric properties were determined by N₂ adsorption at -196°C in a volumetric apparatus (Sorptomatic 1990). Prior to analysis, the sample was outgassed under vacuum at 100°C overnight. Post-processing of the adsorption isotherm according to the Dollimore and Heal method (Dollimore and Heal, 1970) allowed determining the main textural parameters of the K₂CO₃ particles. The porosimetric analysis revealed a prevailing macro-porous nature for the investigated material with a mean pore diameter (d_{pore}) equal to 119 nm. Moreover, the total pore volume (V_p) and the surface area (S_{BET}) are 0.17 cm³ g⁻¹ and 5.9 m² g⁻¹, respectively.

2.2 CO₂ ADSORPTION/REGENERATION TESTS: EXPERIMENTAL APPARATUS AND PROCEDURES

Figure 1 shows a schematic representation of the experimental apparatus adopted for the experimental campaign. The reactor is a fixed-bed column (length=11 cm; inner diameter=2 cm) made up of stainless steel, equipped with a 35 μm porous septum. The fixed-bed temperature was controlled by means of a heating system, arranged coaxially with the adsorber unit. It consists of two 320 W cylindrical shell band heaters (Watlow), enveloped in a thermal insulating layer of stone wool, and connected to PID controllers (i/16 series Omega). The adsorber temperature was monitored *via* a K-type thermocouple.

Pure carbon dioxide was fed to the reactor by means of a mass flow controller (series EI Flow Bronkhorst 201-CV), and mixed with a pre-humidified nitrogen flow to generate a gas mixture of the desired CO₂ concentration. Nitrogen flow rate was measured and controlled by a flow meter. The humidity of the feed gas was set by fluxing

the N₂ stream in a thermostatically-controlled water saturator set at 33°C. Carbon dioxide concentration was measured by a continuous NDIR gas analyzer (AO2020 Uras 26 provided by ABB); data acquisition were performed by interfacing the gas analyzer with a PC via LabView™ software. A CaCl₂ trap was placed at the reactor exit to remove water prior to CO₂ concentration measurements.

Continuous adsorption runs were carried out by feeding the column with a 1.2 L min⁻¹ gas stream containing a 5/5/90% by vol. CO₂/water vapour/N₂ mixture, so to mimic the typical exhaust composition of a marine diesel engine (US-EPA, 2000). The column was loaded with 20 g of K₂CO₃ (previously heated at 110°C for 1 h to remove humidity) diluted in 20 g of inert glass beads (whose particle sizes are comparable with those of the sorbent material). The effect of the operating temperature on the sorbent capture performances was investigated at 60, 75, 90 and 105°C. The time evolution of the composition profile (breakthrough curve) was expressed in terms of the ratio of the volumetric flow rates of CO₂ species at the bed outlet relative to that in the feed $Q_{CO_2}^{out}(t)/Q_{CO_2}^{in}$. From dynamic adsorption tests, it is possible to calculate the amount of CO₂ adsorbed per gram of sorbent at equilibrium, ω^{eq} [mmol g⁻¹], with the following material balance over the adsorption column:

$$\omega^{eq} = \frac{Q_{CO_2}^{in} \rho_{CO_2}}{m M_{CO_2}} \int_0^{t_{eq}} \left(1 - \frac{Q_{CO_2}^{out}(t)}{Q_{CO_2}^{in}} \right) dt$$

(1)

where m is the sorbent dose [g], ρ_{CO_2} [mg L⁻¹] represents the CO₂ density (evaluated at 20°C and 1 bar) while M_{CO_2} is its molecular weight [mg mmol⁻¹]. Finally, t_{eq} [s] is the time required for the gas concentration to practically reach its inlet concentration (outlet concentration approximately equal to 99% of its inlet value). This time is also known as equilibration time.

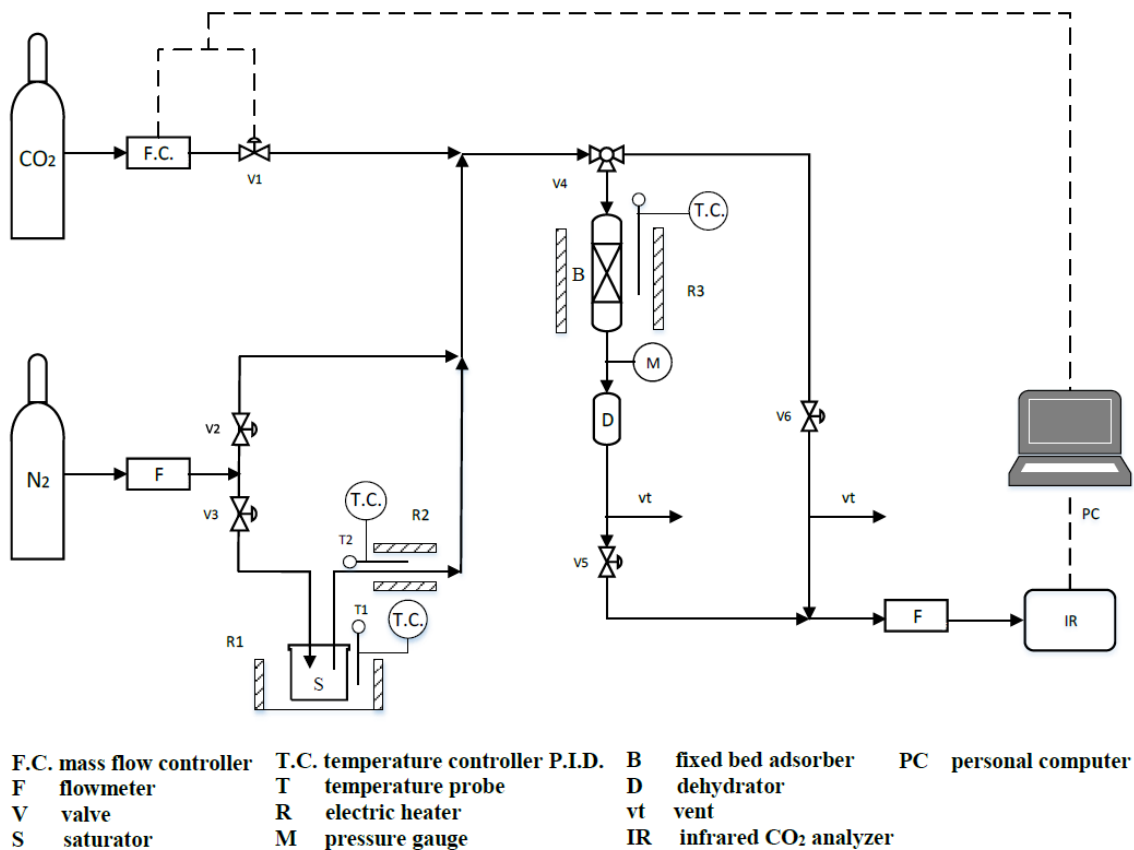


Figure 1: Layout of the experimental apparatus

Desorption runs on the spent K_2CO_3 were performed to investigate the effect of the operating temperature on the recovery dynamics of the adsorbed CO_2 . To this aim, the sorbent was first saturated with CO_2 at $60^\circ C$ under the same sorbent dosage, composition, gas flow rate and pressure conditions described for adsorption tests. After, the fixed-bed column was heated up for 1 h to reach the desired temperature for the desorption stage, and a 1.08 L min^{-1} pure N_2 stream was fed to the reactor as stripping agent. The desorption temperature was fixed at 120, 150, 200, and $250^\circ C$.

The time course of carbon dioxide concentration during the desorption test allowed evaluating the amount of carbon dioxide desorbed from the sorbent, ω^{des} [mmol g^{-1}], through the material balance:

$$\omega^{des} = \frac{P_{CO_2}}{mM_{CO_2}} \int_0^{t_{0.1}} Q_{CO_2}^{out}(t) dt \quad (2)$$

in which $t_{0.1}$ is the time required to complete the desorption process, which corresponds to the NDIR analyser lower detection limit (0.1% CO_2 by vol.).

In order to address the regenerability of the sorbent after an adsorption-desorption cycle, five cycles were performed in sequence by operating with an adsorption temperature of $60^\circ C$ and with desorption temperatures of 120, 150 and $200^\circ C$.

3. RESULTS AND DISCUSSION

3.1 EFFECT OF THE TEMPERATURE ON CO_2 CAPTURE PERFORMANCES

Figure 2 depicts CO_2 breakthrough curves obtained for the K_2CO_3 sorbent at 60, 75, 90 and $105^\circ C$ and under typical naval flue-gas conditions (5/5/90% by vol. CO_2 /water vapour/ N_2 mixture).

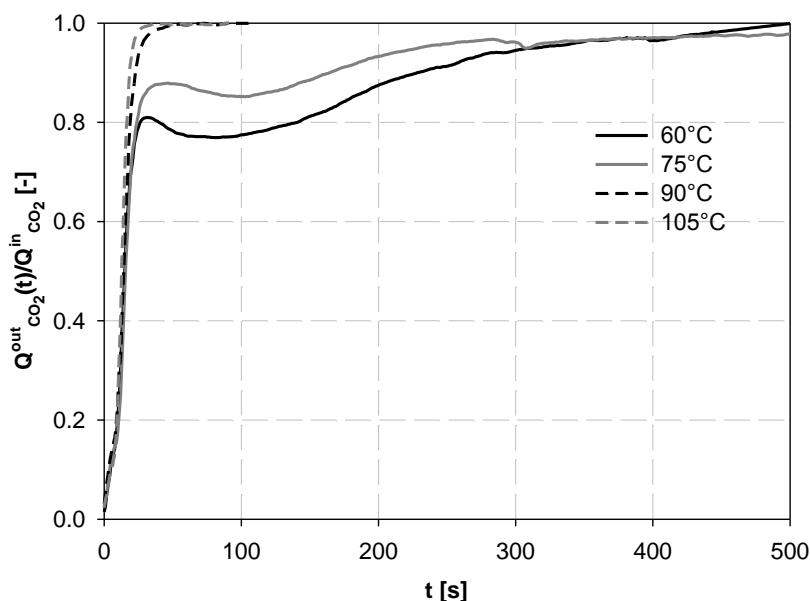


Figure 2: Experimental breakthrough curves obtained for K_2CO_3 at 60, 75, 90 and $105^\circ C$

Results clearly show the significant effect exerted by the operating temperature on the CO_2 capture kinetics. The CO_2 concentration profiles practically overlap at 90 and $105^\circ C$ and the adsorption process is almost complete in 30 s. On the other hand, equilibrium conditions are reached in approximately 450 s for lower adsorption temperatures. At $60^\circ C$, the CO_2 concentration is kept at the lowest level at fixed time, testifying a more efficient capture process. Faster adsorption kinetics at higher temperatures can be ascribed both to an increase in mass transfer rate and to the decrease of the sorbent conversion degree into potassium bicarbonate, due to the exothermic nature of the carbonation process (Ruthven, 1984; Zhao et al, 2012).

Very interestingly, breakthrough curves obtained at 60 and 75°C exhibit a non-monotonic trend with a maximum located approximately at 20 s. This behaviour could be related to a heat release (exothermic process) during the carbonation reaction producing a partial desorption of the captured CO₂. In fact, the increase in the average bed temperature amounted to 3°C for the tests performed at 60 and 75°C, while only 1°C rise was recorded for an initial adsorption temperature of 90°C associated with the disappearance of the concentration peak. At 105°C the system was practically isothermal during the entire test.

The equilibrium adsorption capacity (w^{eq}) determined from post-processing of the dynamic patterns according to Eq. (1) resulted equal to 0.138, 0.116, 0.029 and 0.026 mmol g⁻¹ at 60, 75, 90 and 105°C, respectively. This ranking further confirms the favorable effect of low temperature on the sorbent carbonation degree. This aspect is considered very attractive in the perspective of on board installation of CO₂ after treatment adsorption/desorption units.

In the light of reducing CO₂ emissions deriving from the maritime sector, the best operating conditions for the application of K₂CO₃ sorbent should be selected not only on the basis of its total capture capacity, but also evaluating the characteristic carbonation times allowing a more efficient exploitation of its capture ability. To this end, it is possible to define a CO₂ capture efficiency η [%] as the ratio of the CO₂ flow rate adsorbed in the fixed bed relative to that fed to the reactor. The time dependence of the capture efficiency can be numerically calculated from the kinetic adsorption data according to the following Eq. (3):

$$\eta(t) = \frac{Q_{CO_2}^{in} - Q_{CO_2}^{out}(t)}{Q_{CO_2}^{in}} \quad (3)$$

In turn, this allows computing an average capture efficiency $\bar{\eta}$ at fixed adsorption time t_i defined as:

$$\bar{\eta}(t_i) = \frac{\int_0^{t_i} \eta(t) dt}{t_i}$$

(4)

Table 2 lists the $\bar{\eta}$ values calculated for $t=150, 300$ and 450 s at 60 and 75°C. For higher temperatures, this parameter is not of practical interest due to the very low values of η and to the associated fast decrease in the adsorption efficiency after 30 s.

Table 2: Average capture efficiency for different adsorption times at 60 and 75°C.

Temperature [°C]	$\bar{\eta}$ (150 s)	$\bar{\eta}$ (300 s)	$\bar{\eta}$ (450 s)
60	27.5%	19.2%	14.0%
75	21.9%	14.3%	10.6%

Data analysis reveals that, at each temperature, the average capture efficiency is almost halved from 150 to 450 s. This is related to the marked decrease in the adsorption rate for long test times, also testified by the occurrence of long tails in the breakthrough profiles for $t > 300$ s (Figure 2). Therefore, $\bar{\eta}$ results suggest the possibility of optimizing the sorbent use by stopping the adsorption phase far from equilibrium condition (and switching in desorption mode), because the gain in the sorbent carbonation degree is quite low for times greater than 300 s. Finally, a comparison of $\bar{\eta}$ values for 60 and 75°C, confirms the better capture performances at lower temperature for each considered time, and the differences diminish in the late capture stages.

3.2 SORBENT REGENERATION STUDIES

Figure 3 reports the CO₂ concentration profiles $C_{CO_2}^{out}(t)$ obtained from CO₂ desorption from the spent sorbent (previously saturated with a 5/5/90% by vol. CO₂/water vapour/N₂ mixture at 60°C), carried out in a pure N₂ stream at 120, 150, 200, and 250°C.

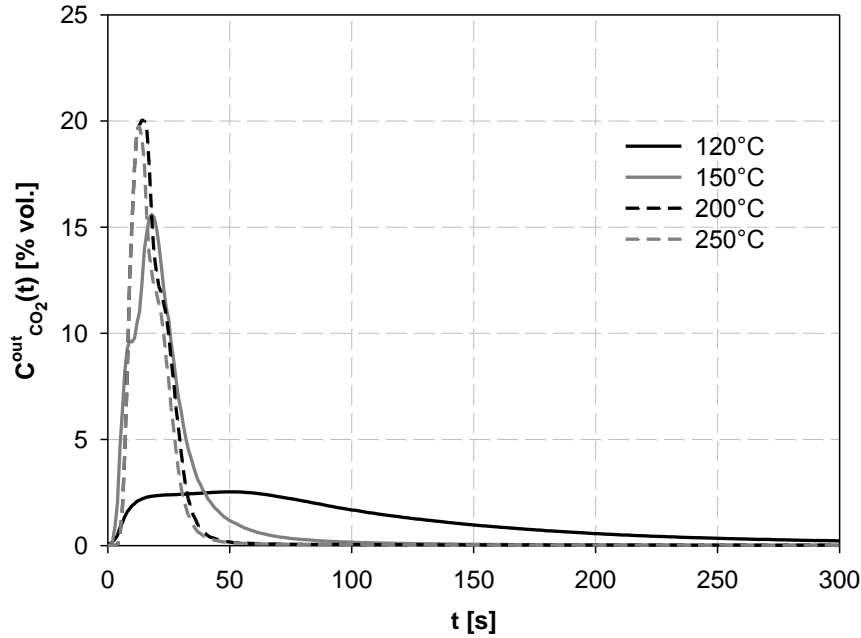


Figure 3: CO₂ desorption profiles obtained at different temperatures

For desorption temperatures greater than 120°C, all the composition patterns reach a peak of CO₂ concentration for short times, indicating that most of CO₂ is quickly desorbed from the sorbent.

At 120°C, the $C_{CO_2}^{out}(t)$ vs t profile shows a hump extended in a wide time range with a maximum concentration recorded of 2.5% by vol., the latter being 15% by vol. at 150°C and 20.5% at both 200 and 250°C. The positive effect induced by an increase in desorption temperature on the CO₂ removal kinetics is also confirmed by a comparison of the total desorption time $t_{0.1}$. In fact, $t_{0.1}$ is 511 s at 120°C, a value 3.8- and 7.7-times greater than those obtained at 150 and 200/250 °C, respectively. The described trends can be related to a faster CO₂ diffusion process occurring at higher temperatures (Ruthven, 1984). Finally, a comparison of ω^{eq} and ω^{des} obtained by working out adsorption and desorption profiles according to Eqs. (1) and (2), allowed checking that, at each desorption temperature, all the adsorbed CO₂ was recovered from spent K₂CO₃ in the first adsorption/desorption cycle (differences were within 2% of the experimental error).

On the basis of the above-discussed desorption results, adsorption-desorption cycles were carried out at desorption temperatures of 120, 150 and 200°C (with a constant adsorption stage performed at 60°C) to preliminary verify the sorbent reusability, which is a critical issue for the practical implementation of an adsorption/desorption unit. Desorption temperatures greater than 200°C were not investigated because, as already mentioned, did not produce an improvement of the CO₂ recovery process both from a kinetic perspective and in terms of average pollutant concentration in the N₂ stripping stream.

Figure 4 (a)-(c) reports a comparison between ω^{eq} and ω^{des} values obtained at different desorption temperatures under 5 adsorption-desorption cycles.

Results demonstrate that for a desorption temperature of 120°C, the adsorption process is completely reversible without any loss of sorbent capture capacity after five cycles. However, this condition is not favorable because of the slow desorption kinetics and of the low CO₂ concentration in the desorption flow with respect to the stream treated in the adsorption phase (Figure 3). When desorption was performed at 150°C, a slight decrease

of adsorption capacity upon the cycles can be observed. In fact, ω^{eq} is 0.135 and 0.110 mmol g⁻¹ for the first and the fifth cycle respectively (corresponding to a 18.5% reduction). Finally, for a desorption temperature of 200°C, the sorbent capture capacity starts to remarkably decrease since the second cycle, and a 51.9% decrease of ω^{eq} can be inferred after 5 cycles. The significant loss in adsorption capacity observed for a desorption temperature of 200°C were justified by a deep modification of the sorbent texture. In particular, a significant reduction of both surface area and porosity with respect to the parent sorbent was observed, determining a reduced accessibility of CO₂ molecules into the pore network just after the first cycle. In fact, V_p and S_{BET} values obtained from N₂ porosimetric analysis on the sorbent after five cycles were 9 and 17 times smaller than the corresponding values retrieved for the raw K₂CO₃.

Considerations hitherto reported suggest that, under the tested operating conditions, a desorption temperature of 150°C represents the most suitable option to recover the adsorbed CO₂, thanks to a good compromise among sorbent cyclability, desorption kinetics and CO₂ concentration in the stripping stream.

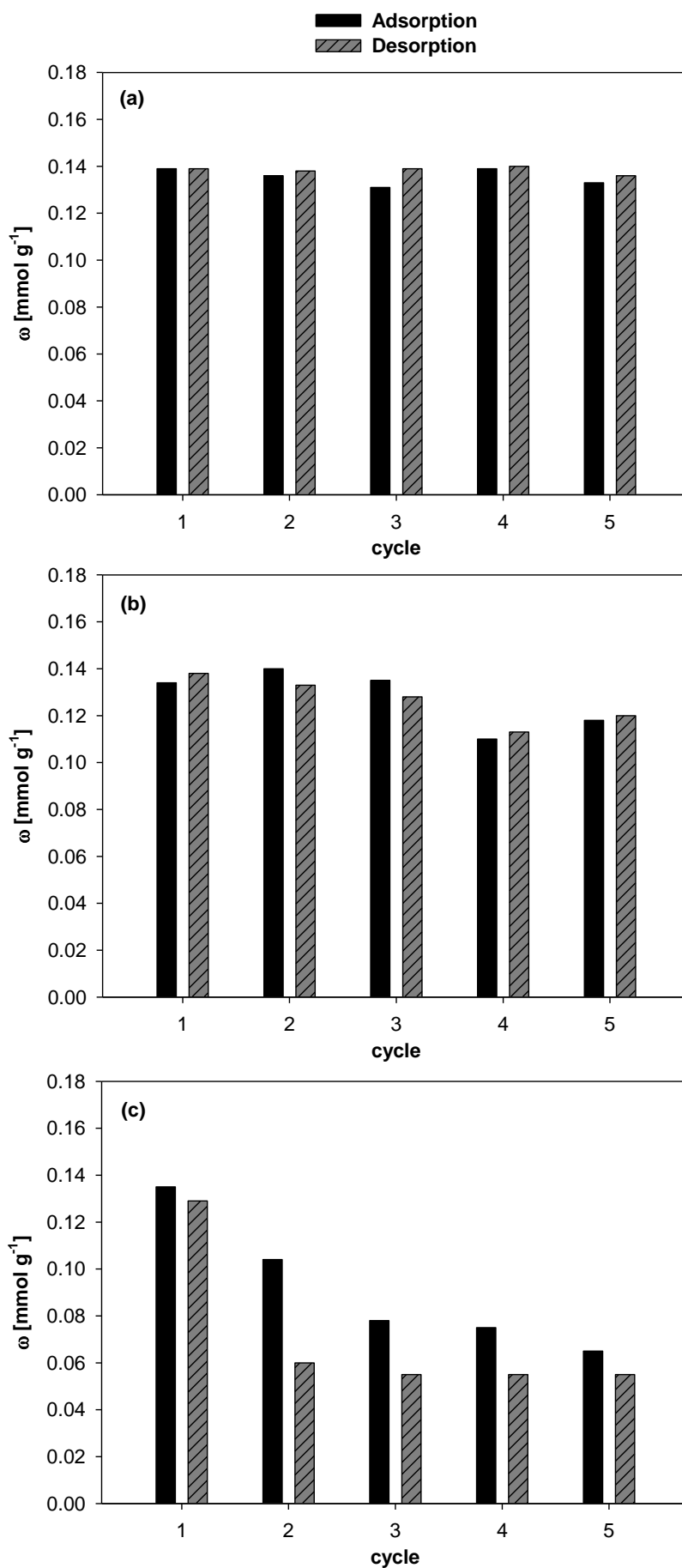


Figure 4: CO₂ adsorption and desorption capacity obtained under 5 adsorption-desorption cycles at desorption temperatures of (a) 120°C, (b) 150°C and (c) 200°C (adsorption step performed at 60°C)

4. CONCLUSIONS

This work is part of a research activity on the depuration of marine Diesel engine exhaust gases, which includes the removal of SO₂, NO_x and PM. After this purification, a last stage of the process may include a carbon dioxide capture and storage step. To this end, our research group is developing a process based on the reaction of potassium carbonate with CO₂.

In this paper, we reported the preliminary results of experiments on CO₂ removal from a model gas stream by simulating the concentration and the temperature of a marine Diesel engine exhaust gas, after the removal of SO₂ and NO_x. The experiments showed that CO₂ removal is more effective at 60°C due to the exothermic nature of the process. Besides, an appreciable regeneration of the spent sorbent can be achieved at 150°C. In this case, the desorption produces a gas stream which contains CO₂ at a more concentrated level than the original exhaust gas if desorption is stopped at short times (i.e. 50 s). In these conditions, the process can be repeated for five cycle with a minimal loss of efficiency for the regenerated sorbent.

The experiments highlighted the potentiality of the proposed process and provided first useful indications for the design of a concept process for CO₂ removal on-board ship.

REFERENCES

Di Natale, F. & Carotenuto, C. (2015). 'Particulate matter in marine diesel engines exhausts: Emissions and control strategies', *Transportation Research Part D: Transport and Environment*, Vol. 40, pp 166-191.

DNV-GL (2013). 'DNV and PSE report on ship carbon capture and storage'. http://www.dnv.com/press_area/press_releases/2013/dnv_and_pse_report_on_ship_carbon_capture__storage.asp

Dollimore, D. & Heal, G.R. (1970). 'Pore-size distribution in typical adsorbent systems', *Journal of Colloid and Interface Science*, Vol. 33, pp 508-519.

EPA (2000). 'Analysis of commercial marine vessels emissions and fuel consumption data'. <http://www3.epa.gov/otaq/models/nonrdmdl/c-marine/r00002.pdf>

International Maritime Organization (2009). 'The Second IMO GHG Study, London'. <http://www.imo.org/en/OurWork/Environment/PollutionPrevention/AirPollution/Documents/GHGStudyFINAL.pdf>

International Maritime Organization (2014). 'Reduction of GHG emissions from ships - Third IMO GHG Study 2014 – Final Report, MEPC 67th session'.

Ruthven, D.M. (1984). 'Principles of adsorption and adsorption processes', New York, John Wiley & Sons.

Waterborne Strategic Research Agenda (2011). <http://www.waterborne-tp.org/index.php/documents>

Waterborne Vision 2025 (2012). <http://www.waterborne-tp.org/index.php/documents>

White paper (2011). 'Roadmap to a single European transport area - Towards a competitive and resource efficient transport system'. http://ec.europa.eu/transport/themes/strategies/2011_white_paper_en.htm

Zhao, C., Chen, X. & Zhao, C. (2012). 'K₂CO₃/Al₂O₃ for capturing CO₂ in flue gas from power plants. Part 1: carbonation behaviors of K₂CO₃/Al₂O₃', *Energy & Fuels*, Vol. 26, 1401-1405.